SEMARAK ILMU PUBLISHING

Journal of Advanced Research in Applied Sciences and Engineering Technology

Journal homepage:
https://semarakilmu.com.my/journals/index.php/applied_sciences_eng_tech/index
ISSN: 2462-1943

Numerical Modelling of a One-dimensional Dam Break Using a Slope-Limiting Positivity-Preserving Discontinuous Galerkin Method

Julius Wang Thye Chuan[1], Mohamad Hidayat Jamal[1], Mohd Ridza Mohd Haniffah[1], Erwan Hafizi Kasiman[1,*]

[1] School of Civil Engineering, Faculty of Engineering, Universiti Teknologi Malaysia (UTM), Johor Bahru 81310, Johor, Malaysia

ABSTRACT

The shallow water equations have been widely used to simulate dam-break problem. Due to the nonlinear and discontinuous nature of the event, application of numerical methods is often plagued with problem such as oscillation and unphysical solutions. The aim of this paper is to simulate a one-dimensional dam break using an improved Discontinuous Galerkin Method. The governing equation is discretized using linear shape function and explicit third-order Runge-Kutta. Problem with negative water depth due to wetting and drying is treated using a combination of thin water layer and min-mod slope limiting techniques. The use of these techniques prevents solution blow-out and oscillation especially at the wet-dry interface. Comparison with available analytical solution shows excellent agreement without under and over-shooting of the solution. Convergence study demonstrate that the overall accuracy of the method is consistent with the shape function order. The method is promising as it can easily be extended to higher order and can be used as an alternative to typical method such as Finite Volume.

Keywords:
Numerical Modeling; Discontinuous Galerkin Method; Shallow Water Equation; Dam Break; Positivity-Preserving

Received: 5 July 2022 | **Revised: 24 July 2022** | **Accepted: 27 July 2022** | **Published: 21 August 2022**

1. Introduction

In recent years, numerical methods have been successfully used to model the dam-break problem. A dam break can be modelled using the three-dimensional Navier Stokes equation, with the free surface treated using a single or multi-phase approach. However, solving the Navier Stokes equation is computationally expensive, especially if the computational domain is large. For practical purposes, the Shallow Water Equations (SWE), a simplified form of the Navier-Stokes equation that consider hydrostatic assumption and a depth-averaged vertical velocity, is usually adopted.

Since dam break is characterized by a discontinuous solution, typical numerical methods, especially those that rely on the continuity between nodes such as the Finite Difference Method (FDM)

* *Corresponding author*
E-mail address: erwanhafizi@utm.my

https://doi.org/10.37934/araset.27.2.115

and Finite Element Method (FEM) struggle to provide an accurate solution for SWE within the discontinuous region. An extremely fine mesh needs to be used to resolve the steep gradient of the solution with upwind technique utilized to reduce oscillations [1, 2]. The implementation of the techniques has undesirable consequences such as an increase in the computational resources and reduction in the overall solution accuracy.

The Finite Volume Method (FVM) is usually used to solve discontinuous problems due to its inherent ability to capture shock. A typical FVM evaluates the derivatives of the governing equation at the center of the cell face [3]. Such evaluation limits the FVM to only second-order accuracy. Although a high-order accuracy can be constructed by evaluating the derivatives at multiple points on the cell face, this increases the complexity of the resulting computational stencils [4]. Recently, the Discontinuous Galerkin Finite Element Method (DGFEM) is introduced as higher order alternative to FVM. The DGFEM combines the shock-capturing ability of the FVM with higher order FEM shape function [5]. The combination allows the DGFEM to model highly discontinuous solutions with an arbitrary solution order [6]. However, the DGFEM still suffers from numerical instabilities such as negative water depth [7]. The negative water depth problem is associated with the wetting and drying of the wavefront, where unphysical water depth is produced, leading to spurious oscillations and blowing-up of the solution [8].

Several techniques, some of which are mostly developed for FVM and FEM, has been proposed for positivity-preserving of the water depth. Some of these techniques are, the mesh adaptation [9, 10], mesh reduction [11, 12] and thin water layer [13-15]. In the mesh adaptation technique, the positivity of the water depth is maintained by matching the mesh with the wet-dry interface. This technique is computationally expensive, especially if the underlying bathymetry is complex, and involves the development of sophisticated algorithm to track the mesh and the wave front [16, 17]. The mesh reduction method tackles the problem by removing cells associated with negative water depth and adding the cells back when the water depth becomes positive [18]. Removing and adding a cell in a computational domain has unfavorable consequences such as loss in momentum and mass, leading to oscillation. Improvement to the technique was introduced by redistributing the mean value of the solution to neighboring cells to improve momentum and mass conservation [19]. However, this then led to significant increase in computational effort.

The thin water layer technique is a simple method that maintain a minimum threshold for dry cell to prevent negative water depth during calculation. Although the technique has issue with mass conservation [20, 21], a slope limiting method can be used to mitigate the issue. Popular slope limiting methods are the min-mod technique [22, 23], the nodal flux method [16], Monotonic Upstream-centered Scheme (MUSCL) [24] and Weighted Essentially Non-Oscillatory (WENO) [25]. The min-mod technique is widely used due to its simplicity and provide a consistent solution when applied to various benchmark cases [26].

Since the DGFEM is relatively new, the application of the method for the solution of SWE in conjunction with various stabilization techniques is quite limited. This paper proposed the use of thin water layer and min-mod techniques for the solution of a 1D dam break problem using DGFEM. This paper starts with the discretization of the SWE using the DGFEM with the stabilizing techniques, followed by the comparison between the numerical solution against analytical solution. Concluding remarks are given in the last section.

2. Methodology

2.1 Governing Equation

The 1D SWE is derived based on the mass and momentum conservation equations, assuming hydrostatic pressure and depth-averaged velocity. The governing equation is given by

$$\frac{\partial h}{\partial t}+\frac{\partial (hu)}{\partial x}=0$$
$$\frac{\partial (hu)}{\partial t}+\frac{\partial \left(hu^2+\frac{1}{2}gh^2\right)}{\partial x}=-gh\frac{\partial b}{\partial x}-gh\frac{n^2(hu)|(hu)|}{h^{\frac{10}{3}}} \quad (1)$$

where h is the water depth, u is the velocity, b is the bed elevation, n is the Manning coefficient, and g is the gravitational acceleration. By introducing q_x as discharge per unit width as follows

$$q_x = hu \quad (2)$$

Eq. (1) can be simplified as:

$$\frac{\partial}{\partial t}Q+\frac{\partial}{\partial x}F(Q)=S_b(Q)+S_f(Q) \quad (3)$$

where

$$\left.\begin{aligned} Q &= \begin{pmatrix} h \\ q_x \end{pmatrix} \\ F(Q) &= \begin{pmatrix} q_x \\ \frac{{q_x}^2}{h}+\frac{1}{2}gh^2 \end{pmatrix} \\ S_b(Q) &= \begin{pmatrix} 0 \\ -gh\frac{\partial b}{\partial x} \end{pmatrix} \\ S_f(Q) &= \begin{pmatrix} 0 \\ -gh\frac{n^2 q_x|q_x|}{h^{\frac{10}{3}}} \end{pmatrix} \end{aligned}\right\} \quad (4)$$

2.2 Spatial and Equation Discretization

Fig. 1 shows the spatial discretization of the discontinuous Galerkin method. Using a linear element with two nodes, the domain is divided into N_e numbers of elements. Note that the adjacent element does not have a shared node as in the typical FEM where element continuity is enforced. Instead, each element in discontinuous at the element interface, with element connectivity enforced through a so-called numerical flux.

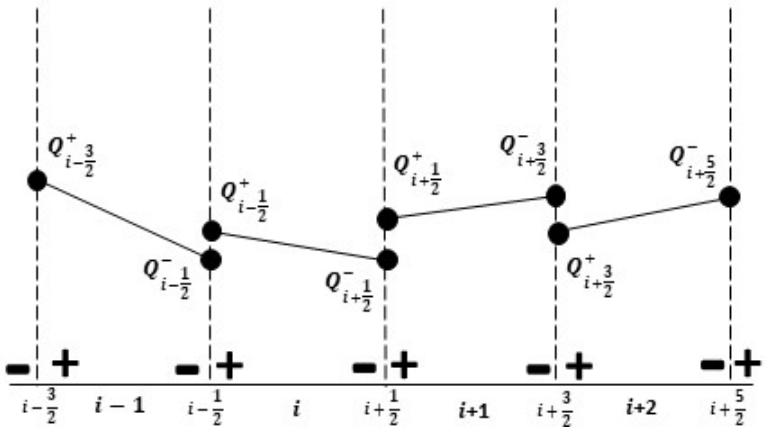

Fig. 1. Spatial discretization of discontinuous Galerkin method

The governing equation given by Eq. (3) is discretized using a standard Galerkin formulation. For each element, the Galerkin formulation is applied by multiplying the governing equation with a weighting function, W, which is then integrated to force the residual of the equation to zero as follows

$$\int_{x_s^e}^{x_e^e} W\left(\frac{\partial Q}{\partial t}+\frac{\partial F(Q)}{\partial x}-S_b(Q)-S_f(Q)\right)dx = 0 \tag{5}$$

The variables in Eq. (5) are approximated by linear shape functions as:

$$\hat{h}=\sum_{i=1}^{n} N_i h_i \qquad \hat{q}_x=\sum_{i=1}^{n} N_i q_{x_i} \tag{6}$$

where n is the total number of nodes in the element and the shape functions for both nodes are

$$N_1=\frac{L-x}{L}, N_2=\frac{x}{L} \tag{7}$$

Substitution of Eq. (6) into Eq. (5) and applying integration by part results in

$$M\frac{\partial \hat{Q}}{\partial t}+\tilde{F}(\hat{Q})-\hat{F}(\hat{Q})=S_b(\hat{Q})+S_f(\hat{Q}) \tag{8}$$

where

$$\left.\begin{aligned} M &= \int_{x_s^e}^{x_e^e} N_i N_j dx \\ \hat{Q} &= \begin{bmatrix} h \\ q_x \end{bmatrix} \\ \tilde{F}(\hat{Q}) &= \begin{bmatrix} N_i \tilde{F}_i^{HLL}(h)\big|_{x_s^e}^{x_e^e} \\ N_i \tilde{F}_i^{HLL}(q)\big|_{x_s^e}^{x_e^e} \end{bmatrix} \\ \hat{F}(\hat{Q}) &= \begin{bmatrix} \int_{x_s^e}^{x_e^e} \frac{\partial N_i}{\partial x} \hat{q}_x dx \\ \int_{x_s^e}^{x_e^e} \frac{\partial N_i}{\partial x} \left(\frac{\hat{q}_x{}^2}{\hat{h}} + \frac{1}{2} g \hat{h}^2 \right) dx \end{bmatrix} \\ S_b(\hat{Q}) &= \begin{bmatrix} 0 \\ -g \int_{x_s^e}^{x_e^e} N_i \hat{h} \frac{\partial b}{\partial x} dx \end{bmatrix} \\ S_f(\hat{Q}) &= \begin{bmatrix} 0 \\ g \int_{x_s^e}^{x_e^e} N_i \left(\frac{n^2 \hat{q}_x |\hat{q}_x|}{\hat{h}^{\frac{10}{3}}} \right) dx \end{bmatrix} \end{aligned}\right\} \quad (9)$$

In Eq. (8), $\hat{Q}$ represents the solution variables, $\hat{F}(\hat{Q})$ represents the flux term, $S_b(\hat{Q})$ represents the bed slope term, and $S_f(\hat{Q})$ represents the friction slope term. $\tilde{F}(\hat{Q})$ represents the numerical flux term for the discontinuous boundary of the elements, where the solution of the numerical flux term can be calculated using the Harten-Lax-Leer (HLL) scheme as follows:

$$\tilde{F}_i^{HLL} = \begin{cases} F^- & if \quad S_L \leq 0 \\ \dfrac{S_R F^- - S_L F^+ + S_L S_R (Q^+ - Q^-)}{S_R - S_L} & if \quad S_L \leq 0 \leq S_R \\ F^+ & if \quad S_R \leq 0 \end{cases} \quad (10)$$

where

$$\left.\begin{aligned} S_L &= \min\left(u^- - \sqrt{gh^-}, u^* - c^*\right) \\ S_R &= \max\left(u^+ + \sqrt{gh^+}, u^* + c^*\right) \\ u^* &= \frac{1}{2}(u^- + u^+) + \sqrt{gh^-} - \sqrt{gh^+} \\ c^* &= \frac{1}{2}\left(\sqrt{gh^-} + \sqrt{gh^+}\right) + \frac{1}{4}(u^- - u^+) \end{aligned}\right\} \quad (11)$$

Note that u^* in Eq. (11) is the wave speed of the node.

2.3 Time Discretization

By applying temporal discretization to Eq. (8), the equation can be written in a compact form as:

$$M \frac{\hat{Q}^{n+1} - \hat{Q}^n}{\Delta t} = R \quad (12)$$

where

$$R = \hat{F}(\hat{Q}) - \tilde{F}(\hat{Q}) + S_b(\hat{Q}) - S_f(\hat{Q})$$

An explicit 3rd order Runge-Kutta method is used to further discretize the temporal terms in Eq. (12) as follows:

$$\left.\begin{aligned} \hat{Q}^{(1)} &= \hat{Q}^n + \Delta t L(\hat{Q}^n) \\ \hat{Q}^{(2)} &= \frac{3}{4}\hat{Q}^n + \frac{1}{4}\hat{Q}^{(1)} + \frac{\Delta t}{4}L(\hat{Q}^{(1)}) \\ \hat{Q}^{n+1} &= \frac{1}{3}\hat{Q}^n + \frac{2}{3}\hat{Q}^{(2)} + \frac{2}{3}\Delta t L(\hat{Q}^{(2)}) \end{aligned}\right\} \quad (13)$$

2.4 Stabilization Schemes

The DGFEM is unstable without stabilization, especially when the portion of the domain is entirely dry. The thin water layer technique is proposed to prevent stability issue. The technique works by making sure that each element is not entirely dry by maintain a co-called threshold water depth, ε_{wet} [21]. Fig. 2 shows the conditions for wet, partially wet, and dry element. If the water depth for all nodes in the element is large than ε_{wet}, the element can be defined as the wet element. If only one of the nodes is above ε_{wet}, it is considered partially wet, while the element is considered dry if both nodes have depths lower than ε_{wet}. In the case of partially wet and dry element, the negative water depth at the node will be converted to the threshold water depth, ε_{wet}, and the velocity for the node is set to zero. This means, there is no redistribution of water depth to the other elements as the element water depth is negative.

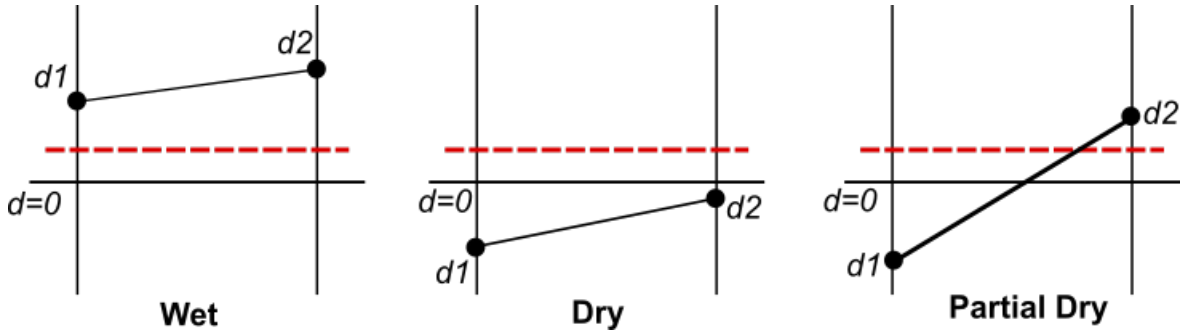

Fig. 2. Representation of wet, dry and partially dry element as compared to threshold water depth (red dashed line).

Since the thin water layer technique does not fully ensure mass convergence, a slope limiter is applied after the water depth treatments to reduce mass loss. The slope limiter is written as

$$Q(x) = \bar{Q} + (x - \bar{x})\sigma \; for \; x_s^e < x < x_e^e \quad (14)$$

where $\bar{Q}$ is the average value of the variable for element, $\bar{x}$ is the midpoint of the element, and σ is the slope limiter parameter. In this study, a simple min-mod slope limiter parameter is used. The slope limiter function is given by the following equation

$$\sigma = \left[\frac{sign(a) + sign(b)}{2}\right] min\ (|a|, |b|) \tag{15}$$

in which

$$\left.\begin{aligned} a &= \frac{\bar{Q}_{i+1} - \bar{Q}_{i-1}}{\bar{x}_{i+1} - \bar{x}_{i-1}} \\ b &= \frac{\bar{Q}_{i+1} - \bar{Q}_{i-1}}{\bar{x}_{i+1} - \bar{x}_{i-1}} \end{aligned}\right\} \tag{16}$$

2.5 Dam Break Description

The dam-break considered for this study consists of domain with varying water depth at the upstream and downstream sections, separated by a vertical dam at the middle [27]. The difference between upstream and downstream water depths produces a discontinuity at the interface between upstream and downstream sections. The 1D dam-break was modelled for both the wet bed and dry bed cases. The latter used to investigate the influence of wetting and drying on the solution. Fig. 3 shows the schematic view of the initial condition for the wet bed and dry bed dam-break cases.

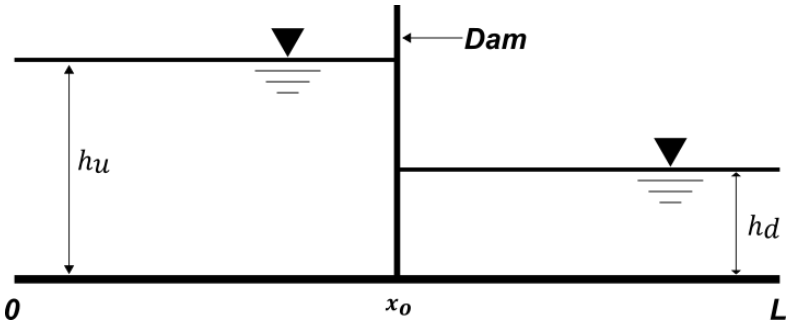

Fig. 3. Initial condition for the dam break problem

In this study, the computational domain has a length of $L = 600\ m$, and the dam is located at $x_0 = 300\ m$. The initial upstream water depth for wet bed and dry bed dam-break cases were similar with value of $h_u = 10\ m$. The downstream water depth for the wet bed dam break case is set to $1\ m$, while zero water depth is used for the dry bed case. The numerical case was modelled with an element size of 24 m, 12 m, 6 m, 3 m and 1.5 m. The numerical cases of wet and dry bed dam-break were modelled using a fixed time steps for all cases. The numerical solution is compared with the exact solution by Wu *et al.* [28].

2.6 Initial and Boundary Conditions

For the dam-break case, the initial condition is prescribed for the upstream, h_u , and downstream, h_d, water depths. The flow rate is set to zero for the whole domain during the start of the simulation. An open boundary condition is used at both ends, where water is allowed to escape from the domain. The initial and boundary conditions can be summarized as follows

$$\begin{aligned} h(x,0) &= \begin{cases} h_u \text{ if } x \le x_0 \\ h_d \text{ if } x > x_0 \end{cases} \\ q(x,0) &= 0 \\ \frac{\partial h}{\partial x}(0,t) = \frac{\partial h}{\partial x}(L,t) = \frac{\partial q}{\partial x}(0,t) = \frac{\partial q}{\partial x}(L,t) &= 0 \end{aligned} \tag{17}$$

where x_0 is the location of the dam and L is the length of the domain.

2.7 Error Analysis

The error between numerical result and analytical solution calculated based on L^2-norm [29]. The error can be calculated by the quadrature rule for the integral. The integral of equation can be summarized as follows:

$$\|u - u_h\|_{L_2}^2 = \sum_{i=1}^{N} \sum_{q=1}^{N_q} \left(u(x_q) - u_h(\hat{x}_q)\right)^2 \hat{w}_q |J| \tag{18}$$

where u is the exact solution, u_h is the numerical solution, $\hat{x}_q$ is the Gauss point, $\hat{w}_q$ is the Gauss weight and J is the Jacobian.

3. Results and Discussion

3.2 Wet Bed Dam Break Case

A convergence study was carried out to ensure that the solution is mesh independent. Table 1 shows the summary of L^2-norm error of the water depth and flow rate for the wet bed dam-break with different mesh sizes. Fig. 4 presents the convergence plot for the wet bed dam-break case. The water depth and flow rate errors show reduction as the element size decreases. From the plot, the convergence rates for both water depth and flow rate are given as first order. The correlation coefficient, R^2 values is close to 1 for the water depth and flow rate results, highlighting the accuracy of the numerical solution.

Fig. **5** shows the water depth results for different time steps between the numerical result and analytical solution with close-up views of the water depth given by Fig. 5(b) and Fig. 5(c). Overall, the agreement between the numerical and analytical solution is excellent. At the discontinuous region, slight differences between the numerical and analytical solution can be observed. However, the numerical solution shows no over-shooting and under-shooting of the result.

Fig. 6 shows the results of the flow rate for different time steps between the numerical result and analytical solution. The numerical results agree with the exact solution, particularly for the region away from the discontinuity. Fig. **6**(b) and Fig. **6**(c) show the zoomed in view of the result. The same deviation can be found on the flow rate curves, especially at the initial state of the curves and the peak of the curves. Far from the discontinuous region, excellent agreement of the result without any overshoot and undershoot is observed.

Table 1
L^2-norm error for wet bed dam break

Element Size, m	Water depth error	Flow rate error
24.00	0.0914	0.2670
12.00	0.0480	0.1323
6.00	0.0213	0.0483
3.00	0.0093	0.0217
1.50	0.0052	0.0154

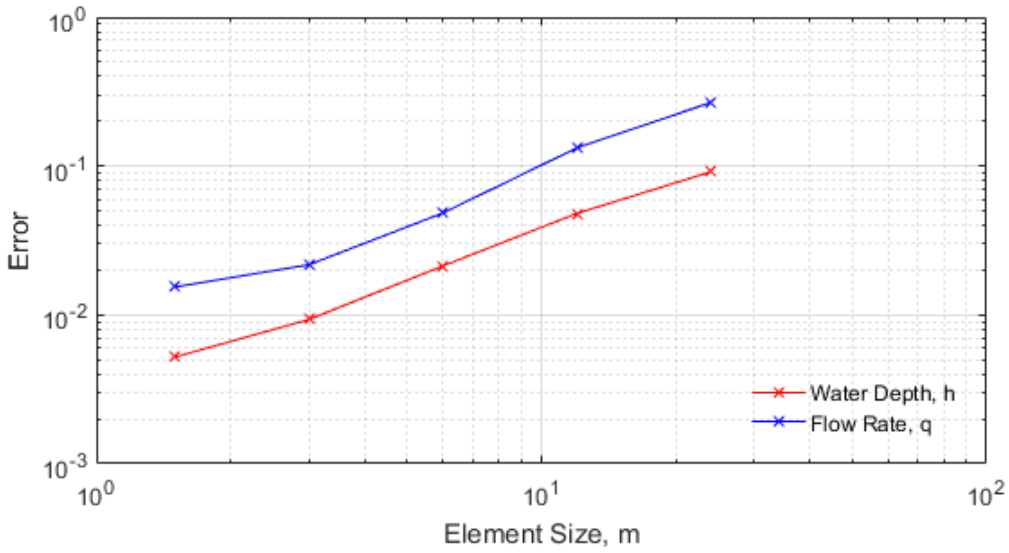

Fig. 4. Convergence plot of wet bed dam break case

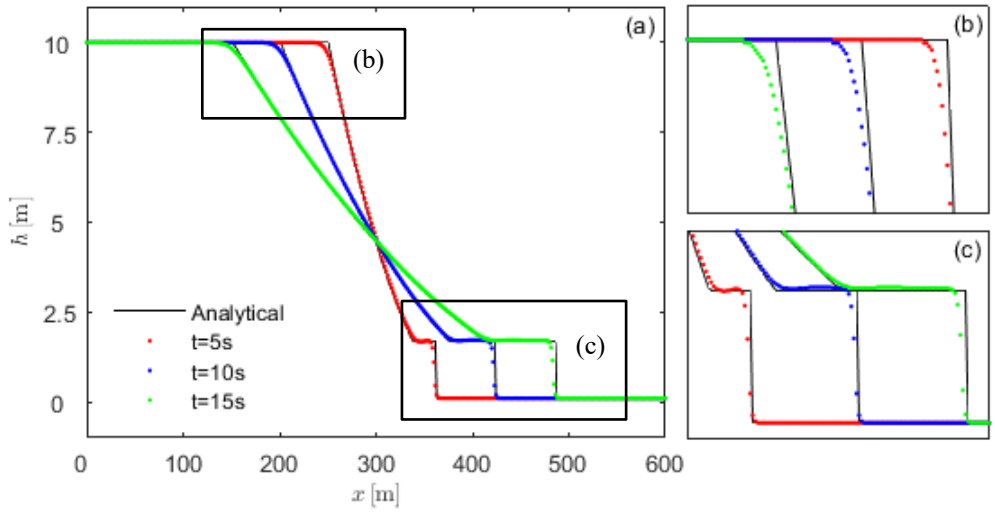

Fig. 5. Water depth between the numerical and analytical solution at different time step for wet bed dam break over (a) entire domain (b) 100m<x<275m (c) 325m<x<500m

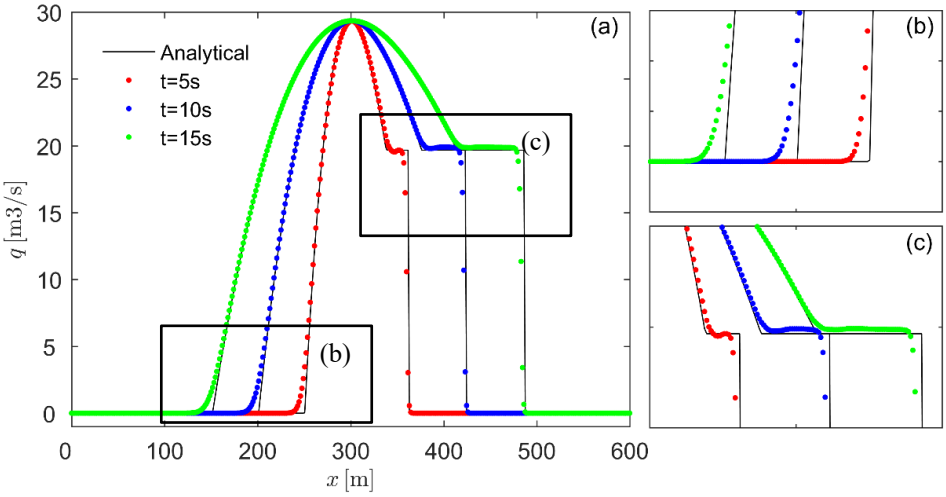

Fig. 6 Flow rate between the numerical and analytical solution at different time step for wet bed dam break over (a) entire domain (b) 100m<x<275m (c) 325m<x<500m

3.3 Dry Bed Dam Break Case

Table 2 shows the summary the solution error while Fig. 7 presents the convergence plot for the dry bed dam-break case. Similar to the wet dam break case, the error of the solution reduces with the decrease in element sizes. The convergence rates of the water depth and flow rate are first order. The correlation R^2 values is close to unity, showing excellent agreement between numerical result and analytical solutions.

Fig. 8 and 9 show the water depth and flow rate results for the dry dam break case at various time steps. Although the case starts with portion of the domain completely dry, the DGFEM can provide a stable and accurate solution. The result shows that the agreement between the numerical and exact solutions is excellent for region far from the discontinuity. Focusing on the discontinuous region, as shown in Figs. 8 (b) and 8(c), slight discrepancies can be observed. Owing perhaps to the slope limiter scheme, the model is able to prevent any over shooting and under shooting of the result.

Table 2
L^2-norm error for dry bed dam break

Element Size, m	Water depth error	Flow rate error
24.00	0.0049	0.0125
12.00	0.0027	0.0063
6.00	0.0011	0.0029
3.00	0.0005	0.0014
1.50	0.0002	0.0006

3.4 The Importance of Positivity Preserving Scheme

Previous section shows excellent agreement between the numerical result and analytical solution with no instability issue. The stability of the numerical solution is partly achieved due to the inclusion of the positivity-preserving scheme. This section examines the result of the model without the positivity-preserving scheme to highlight the importance of the scheme in providing stable solution. Results for the water depth and flow rate without the positivity-preserving scheme as compared to

analytical solution are presented in Fig. 10 and Fig. 11. The plot is produces at a time step of $t = 1$s, just before at the solutions blows. It can be seen that over and under-shooting of the solution clearly evident at the discontinuous region as shown in Fig. 10 (b) and (c). Negative water depth starts to develop at the downstream part. The solution is becoming more severe for the flow rate as the value starts to become exceedingly large at the downstream section (Fig. 11 (b) and (c)). As the error increases for each time step, the solution become unstable and blows [8]. The plot of maximum error for water depth and flow rate is given by Fig. 12. The plot shows that the solution blows after $t = 1$s.

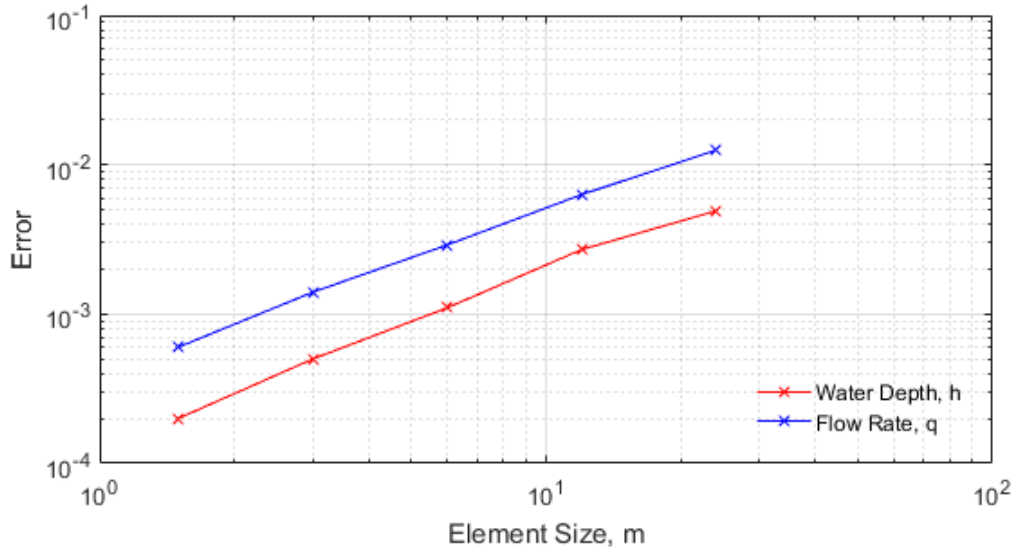

Fig. 7. Convergence plot of dry bed dam break case

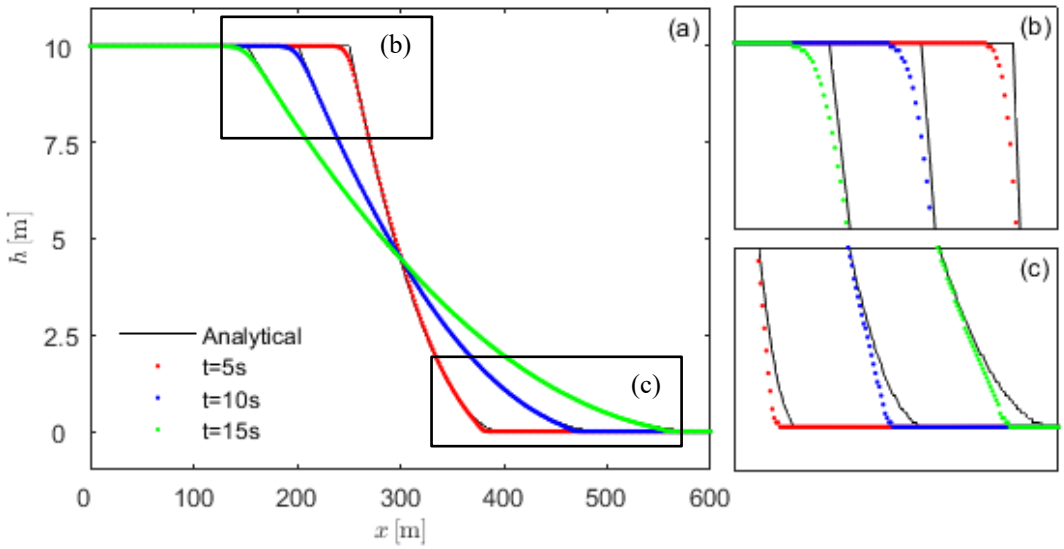

Fig. 8. Water depth between the numerical and analytical solution at different time step for dry bed dam break over (a) entire domain (b) 100m<x<275m (c) 350m<x<600m

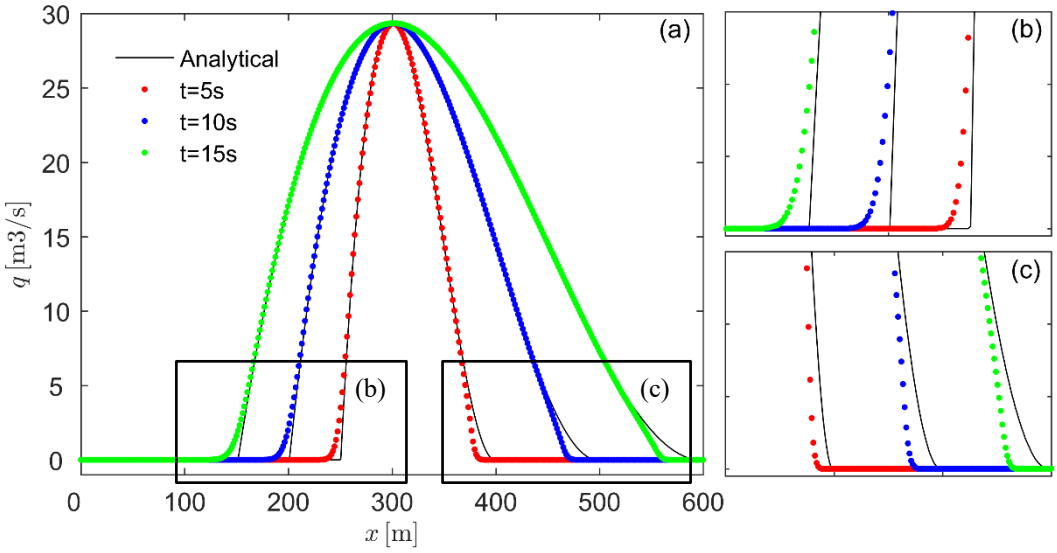

Fig. 9. Flow rate between the numerical and analytical solution at different time step for dry bed dam break over (a) entire domain (b) 100m<x<275m (c) 350m<x<600m

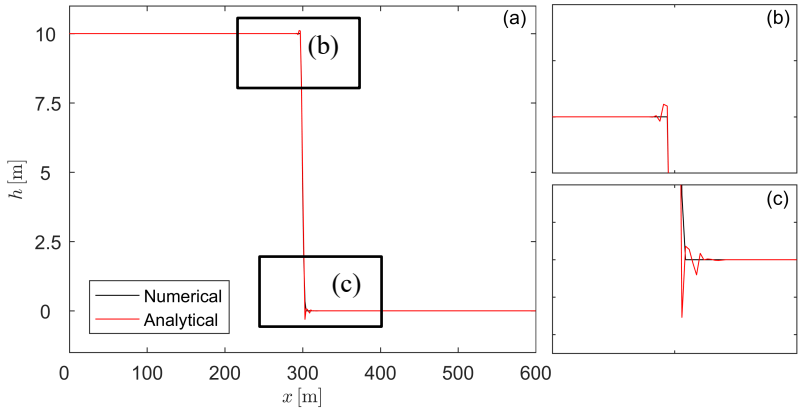

Fig. 10 Water depth between analytical and numerical (without positivity-preserving scheme) over (a) entire domain (b) 280m<x<320m (c) 280m<x<320 at time step of $\boldsymbol{t = 1}$s

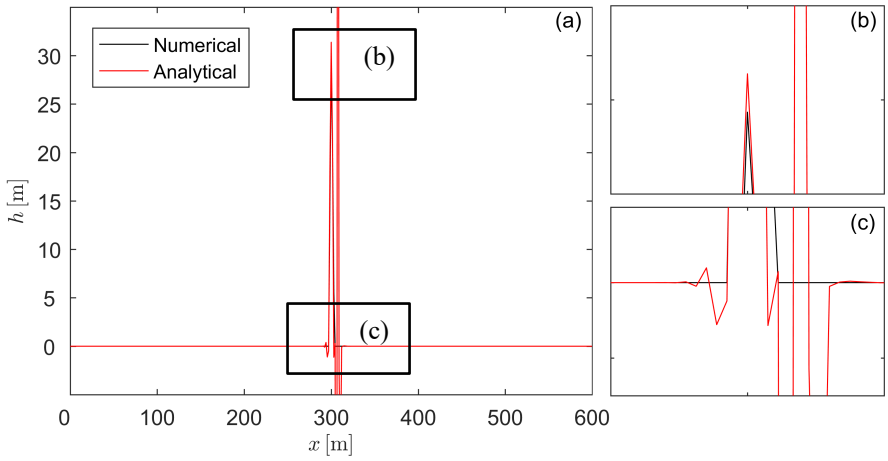

Fig. 11 Flow rate between analytical and numerical (without positivity-preserving scheme) over (a) entire domain (b) 280m<x<320m (c) 280m<x<320m at time step of $\boldsymbol{t = 1}$s

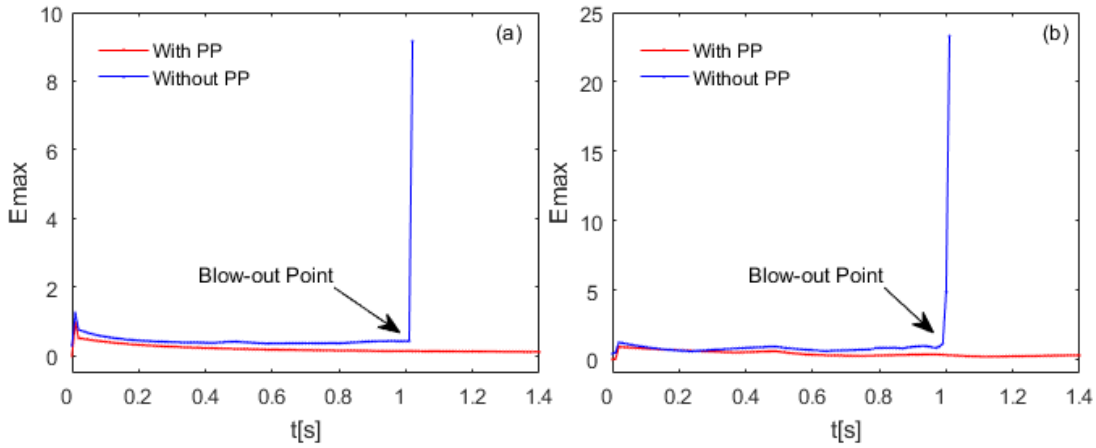

Fig. 12 Maximum error of with and without positivity-preserving scheme (PP) before blow-out for (a) water depth and (b) flow rate

Without any stabilization scheme, the numerical model produces an unphysical, negative water depth especially when the bed is dry. The generation of negative water depth is problematic since the calculation of the numerical flux required the evaluation of the square root of the water depth (the term $\sqrt{gh}$). The thin water layer technique used in this study is proven to be critical to achieve a stable solution. The scheme always ensure that each element is wet and prevent any over and under-shooting of the solution that could potentially generate a negative water depth [30].

4. Conclusions

In this paper, an improved DGFEM has been successfully developed for the solution of a 1D dam-break by combining the thin water later and min-mod stabilization techniques. With the stabilization techniques, comparison between numerical and analytical solution shows excellent agreement for wet and dry dam break cases. With the stabilization techniques removed, the solution of the dry dam break quickly blows, highlighting the importance of preserving the positivity of the water depth.

Acknowledgement

This research was funded by a grant from Universiti Teknologi Malaysia (PY/2020/03511).

References

[1] Wang, Xiufang, Gang Li, Shouguo Qian, Jiaojiao Li, and Zhen Wang. "High order well-balanced finite difference WENO schemes for shallow water flows along channels with irregular geometry." *Applied Mathematics and Computation* 363 (2019): 124587. https://doi.org/10.1016/j.amc.2019.124587

[2] Li, Peng, Wai Sun Don, and Zhen Gao. "High order well-balanced finite difference WENO interpolation-based schemes for shallow water equations." *Computers & Fluids* 201 (2020): 104476. https://doi.org/10.1016/j.compfluid.2020.104476

[3] Moukalled, Fadl, Luca Mangani, and Marwan Darwish. "The finite volume method." In *The finite volume method in computational fluid dynamics*, pp. 103-135. Springer, Cham, 2016. https://doi.org/10.1007/978-3-319-16874-6_5

[4] Hesthaven, Jan S., and Tim Warburton. *Nodal discontinuous Galerkin methods: algorithms, analysis, and applications*. Springer Science & Business Media, 2007. https://doi.org/10.1007/978-0-387-72067-8

[5] Zhu, Jun, Chi-Wang Shu, and Jianxian Qiu. "High-order Runge-Kutta discontinuous Galerkin methods with a new type of multi-resolution WENO limiters on triangular meshes." *Applied Numerical Mathematics* 153 (2020): 519-539. https://doi.org/10.1016/j.apnum.2020.03.013

[6] Liu, Yilang, Weiwei Zhang, and Xiaobo Zheng. "An accuracy preserving limiter for the high-order discontinuous Galerkin method on unstructured grids." *Computers & Fluids* 192 (2019): 104253. https://doi.org/10.1016/j.compfluid.2019.104253

[7] Xing, Yulong, and Chi-Wang Shu. "A survey of high order schemes for the shallow water equations." *J. Math. Study* 47, no. 3 (2014): 221-249. https://doi.org/10.4208/jms.v47n3.14.01

[8] Vater, Stefan, Nicole Beisiegel, and Jörn Behrens. "A limiter-based well-balanced discontinuous Galerkin method for shallow-water flows with wetting and drying: Triangular grids." *International Journal for Numerical Methods in Fluids* 91, no. 8 (2019): 395-418. https://doi.org/10.1002/fld.4762

[9] Christian, C. D., and G. N. Palmer. "A deforming finite element mesh for use in moving one-dimensional boundary wave problems." *International journal for numerical methods in fluids* 25, no. 4 (1997): 407-420. https://doi.org/10.1002/(SICI)1097-0363(19970830)25:4<407::AID-FLD556>3.0.CO;2-6

[10] Prasad, R. S., and I. A. Svendsen. "Moving shoreline boundary condition for nearshore models." *Coastal engineering* 49, no. 4 (2003): 239-261. https://doi.org/10.1016/S0378-3839(03)00050-4

[11] Greenberg, David A., Jennifer A. Shore, Fred H. Page, and Michael Dowd. "A finite element circulation model for embayments with drying intertidal areas and its application to the Quoddy region of the Bay of Fundy." *Ocean Modelling* 10, no. 1-2 (2005): 211-231. https://doi.org/10.1016/j.ocemod.2004.06.005

[12] Dietrich, J. C., R. L. Kolar, and J. J. Westerink. "Refinements in continuous Galerkin wetting and drying algorithms." In *Proc. Ninth Int. Conf. on Estuarine and Coastal Modeling*, pp. 637-656. 2006. https://doi.org/10.1061/40876(209)37

[13] Chen, Changsheng, Jianhua Qi, Chunyan Li, Robert C. Beardsley, Huichan Lin, Randy Walker, and Keith Gates. "Complexity of the flooding/drying process in an estuarine tidal-creek salt-marsh system: An application of FVCOM." *Journal of Geophysical Research: Oceans* 113, no. C7 (2008). https://doi.org/10.1029/2007JC004328

[14] Rego, J. L., and C. Li. "On the receding of storm surge along Louisiana's low-lying coast." *Journal of Coastal Research* (2009): 1045-1049. https://www.jstor.org/stable/25737946

[15] Zhao, Liuzhi, Changsheng Chen, Joe Vallino, Charles Hopkinson, Robert C. Beardsley, Huichan Lin, and Jim Lerczak. "Wetland-estuarine-shelf interactions in the Plum Island Sound and Merrimack River in the Massachusetts coast." *Journal of Geophysical Research: Oceans* 115, no. C10 (2010). https://doi.org/10.1029/2009JC006085

[16] Gourgue, Olivier, Richard Comblen, Jonathan Lambrechts, Tuomas Kärnä, Vincent Legat, and Eric Deleersnijder. "A flux-limiting wetting–drying method for finite-element shallow-water models, with application to the Scheldt Estuary." *Advances in Water Resources* 32, no. 12 (2009): 1726-1739. https://doi.org/10.1016/j.advwatres.2009.09.005

[17] Bokhove, Onno. "Flooding and drying in discontinuous Galerkin finite-element discretizations of shallow-water equations. Part 1: one dimension." *Journal of scientific computing* 22, no. 1 (2005): 47-82. https://doi.org/10.1007/s10915-004-4136-6

[18] Medeiros, Stephen C., and Scott C. Hagen. "Review of wetting and drying algorithms for numerical tidal flow models." *International journal for numerical methods in fluids* 71, no. 4 (2013): 473-487. https://doi.org/10.1002/fld.3668

[19] Martins, Ricardo, Jorge Leandro, and Slobodan Djordjević. "Wetting and drying numerical treatments for the Roe Riemann scheme." *Journal of Hydraulic Research* 56, no. 2 (2018): 256-267. https://doi.org/10.1080/00221686.2017.1289256

[20] Xing, Yulong, Xiangxiong Zhang, and Chi-Wang Shu. "Positivity-preserving high order well-balanced discontinuous Galerkin methods for the shallow water equations." *Advances in Water Resources* 33, no. 12 (2010): 1476-1493. https://doi.org/10.1016/j.advwatres.2010.08.005

[21] Lee, Haegyun, and Namjoo Lee. "Wet-dry moving boundary treatment for Runge-Kutta discontinuous Galerkin shallow water equation model." *KSCE Journal of Civil Engineering* 20, no. 2 (2016): 978-989. https://doi.org/10.1007/s12205-015-0389-x

[22] Mungkasi, Sudi, and Stephen G. Roberts. "On the best quantity reconstructions for a well balanced finite volume method used to solve the shallow water wave equations with a wet/dry interface." *Anziam Journal* 51 (2009): C48-C65. https://doi.org/10.21914/anziamj.v51i0.2576

[23] Zhang, MingLiang, YuanYuan Xu, ZiNing Hao, and Yang Qiao. "Integrating 1D and 2D hydrodynamic, sediment transport model for dam-break flow using finite volume method." *Science China Physics, Mechanics and Astronomy* 57, no. 4 (2014): 774-783. https://doi.org/10.1007/s11433-013-5294-z

[24] Kesserwani, Georges, and Qiuhua Liang. "Well-balanced RKDG2 solutions to the shallow water equations over irregular domains with wetting and drying." *Computers & Fluids* 39, no. 10 (2010): 2040-2050. https://doi.org/10.1016/j.compfluid.2010.07.008

[25] Zhang, Xiangxiong, and Chi-Wang Shu. "On maximum-principle-satisfying high order schemes for scalar conservation laws." *Journal of Computational Physics* 229, no. 9 (2010): 3091-3120. https://doi.org/10.1016/j.jcp.2009.12.030

[26] Vater, Stefan, Nicole Beisiegel, and Jörn Behrens. "A limiter-based well-balanced discontinuous Galerkin method for shallow-water flows with wetting and drying: One-dimensional case." *Advances in water resources* 85 (2015): 1-13. https://doi.org/10.1016/j.advwatres.2015.08.008

[27] French, Richard H., and Richard H. French. *Open-channel hydraulics*. New York: McGraw-Hill, 1985. https://heidarpour.iut.ac.ir/sites/heidarpour.iut.ac.ir/files/u32/open.pdf

[28] Wu, Chao, Guofu Huang, and Yonghong Zheng. "Theoretical solution of dam-break shock wave." *Journal of Hydraulic Engineering* 125, no. 11 (1999): 1210-1215. https://doi.org/10.1061/(ASCE)0733-9429(1999)125:11(1210)

[29] Wang, Qiuliang, and Jinru Chen. "An unfitted discontinuous Galerkin method for elliptic interface problems." *Journal of Applied Mathematics* 2014 (2014). https://doi.org/10.1155/2014/241890

[30] Mao, Jia, Lanhao Zhao, Xin Bai, Bowen Guo, Zhi Liu, and Tongchun Li. "A novel well-balanced scheme for modeling of dam break flow in drying-wetting areas." *Computers & Fluids* 136 (2016): 324-330. https://doi.org/10.1016/j.compfluid.2016.06.022